THE ASTRONOMICAL JOURNAL VOLUME 85, NUMBER 10 OCTOBER 1980

HOW TO OBTAIN THE TRUE CORRELATION FROM A 3-LEVEL DIGITAL CORRELATOR

SHRINIVAS R. KULKARNI and CARL HEILES
Astronomy Department, University of California at Berkeley, Berkeley, California 94720
Received 14 April 1980; revised 16 June 1980

ABSTRACT

A set of explicit approximation formulas to relate correlation as measured by a 3-level digital autocorrelator to the true correlation has been developed. These formulas are accurate to much less than 0.5%, and are also applicable to the more general case of a cross correlator. With the help of numerical simulations, the effects of the drifts of the transition levels on the power spectrum and the inaccuracy of the formulas have been studied. In the cases studied, which are representative of practical applications, the deviations from the scaling are less than 0.5% of the peak signal. We conclude that the inaccuracies inherent in the reduction methods and drifts in transition levels do not give rise to any significant errors in observed power spectra.

I. INTRODUCTION

Three-level digital correlators are being increasingly used in radio astronomy, and have entirely displaced one-bit correlators in modern designs. Many properties of these correlators have been considered theoretically by Cooper (1970), Hagen and Farley (1973), Bowers and Klinger (1974), and Thompson (1973). In this paper we derive convenient approximations to, and consider the accuracy required of, the numerical conversion of the measured correlation to the true correlation function.

A 3-level correlator quantizes the input signal $V(t)$ into levels -1, 0, or 1, depending on whether $V(t)$ lies, respectively, between $-\infty$ and the negative transition level $a\sigma$, between $a\sigma$ and the positive transition level $c\sigma$, or between $c\sigma$ and ∞. Here σ is the rms input voltage. This quantization is represented by a transfer function, $g(V(t))$; from the standpoint of signal-to-noise ratio, the optimum values of $|a|$ and c are 0.6120 (Thompson 1973).

Let $r(z)$ be the autocorrelation function of $V(t)$, as measured by a 3-level correlator. Let $\rho(z)$ be the corresponding quantity which would be measured by a perfect analog correlator. Then,

$$\rho(z) \propto \langle V(t)V(t+z)\rangle,$$
$$r(z) \propto \langle g(V(t))g(V(t+z))\rangle, \qquad (1)$$

where the brackets indicate time average. Hereinafter, we assume that ρ is normalized, i.e., $\rho(0) = 1$, and that $r(z)$ is the ratio of the counts in channel with delay z to the total number of samples performed. The relation between $\rho(z)$ and $r(z)$ depends on the statistics of the signal. If $V(t)$ is Gaussian random noise, as is always assumed in radio astronomy, then

$$r(z) - r(\infty) = (2\pi)^{-1} \int_0^{\rho(z)} dx(1-x^2)^{-1/2}(\exp[-c^2/(1+x)] + \exp[-a^2/(1+x)] + 2\exp\{(2acx - a^2 - c^2)/[2(1-x^2)]\}). \qquad (2)$$

This is a simple extension of the results of Hagen and Farley (1973), who considered the case $-a = c$ only; $r(\infty)$ is zero only when $-a = c$.

II. APPROXIMATIONS TO EQ. (2)

Equation (2) cannot be represented exactly in closed form. We have developed approximations for two ranges of $\rho(z)$ by the methods outlined in Appendix A. The lower inversion approximation, valid for $|\rho| < 0.86$, can be carried to arbitrary order; the upper inversion approximation, valid for $|\rho| > 0.86$, involves the solution of a transcendental equation.

In Sec. III we consider the accuracy required of the approximations. We find that in practice it is sufficient to use the lower inversion approximation of order 3 together with the upper inversion approximation of order zero. For the case $-a = c$, these approximations are

$$\rho(z) = Ar + Br^3, \qquad |\rho| < 0.86, \qquad (3)$$

where

$$A = (\pi/2)\exp(c^2),$$
$$B = -A^3[(c^2-1)^2/6]$$

and

$$\rho(z) = \mathrm{sgn}[r(z)]\cos\{\pi[r(0) - |r(z)|]\exp(c^2/2)\}, \qquad |\rho| > 0.86. \qquad (4)$$

A rough estimate of $\rho(z)$ is given by $\rho = Ar$. Some examples of errors of this approximation, including some cases when $-a \neq c$, are shown in Figs. 1(a) and 1(b).

The transition level c is easily obtainable from $r(0)$. At $z = 0$, the only possible results of the product $g(V(t))$ are 0 and 1; 1 occurs when $|V(t)| > c$. Thus, $r(0)$ is simply

$$r(0) = 1 - \mathrm{erf}(c/\sqrt{2}). \qquad (5)$$

With the help of an approximation due to Hastings (1966), c can be obtained directly from $r(0)$; the accu-

 0004-6256/80/101413-08$00.90

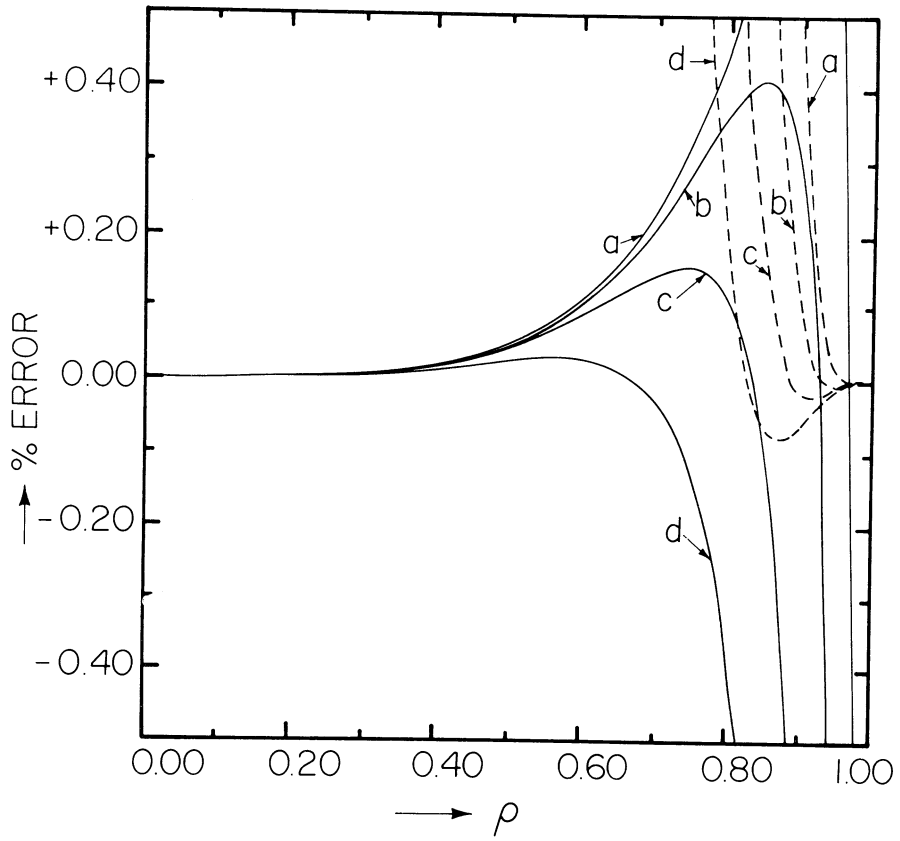

FIG. 1(a). The solid curve represents the % error of the lower inversion approximation of order 3, and the dashed curve is the upper inversion formula of order zero; the % error is defined to be $100[(\rho - \rho_{calculated})/\rho]$. Curve "a" refers to the case $-a = c = 0.41$, curve "b" to $-a = c = 0.51$, curve "c" to $-a = c = 0.61$, and curve "d" to $-a = c = 0.71$.

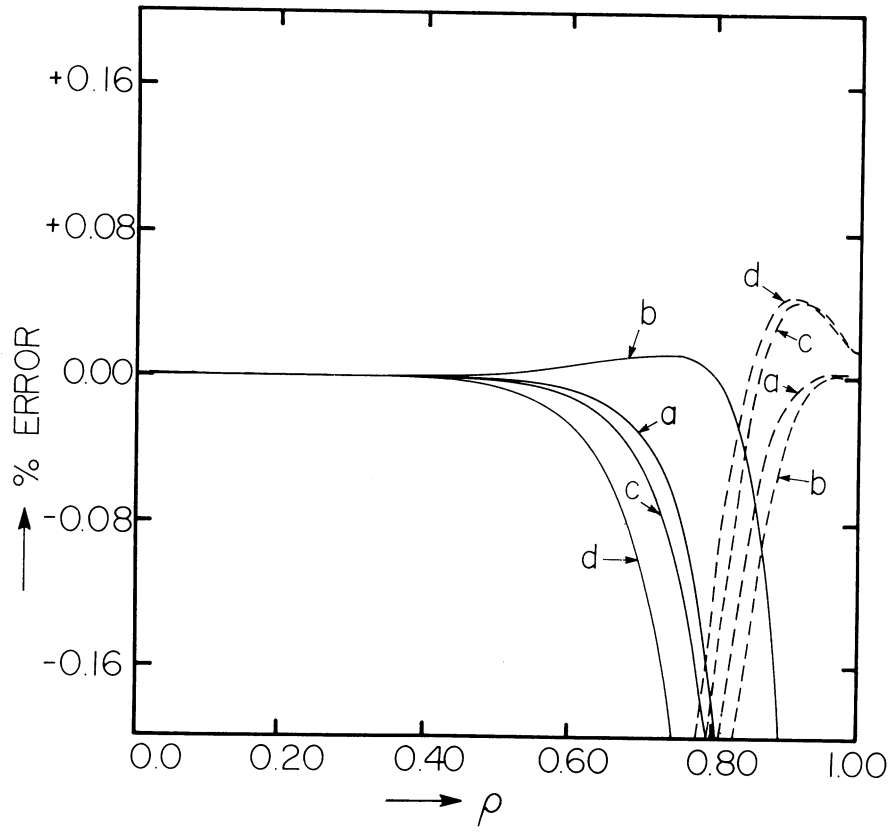

FIG. 1(b). The solid curve represents % error of the lower inversion approximation of order 5, and the dashed curve the upper inversion formula with one iteration of the Newton-Ralphson method; the % error is defined the same way as in Fig. 1(a). Curve "a" refers to the case $-a = c = 0.61$; curve "b" to $-a = c = 0.51$; curve "c" to $-a = 0.60$, $c = 0.65$; and curve "d" to $-a = 0.60$, $c = 0.70$.

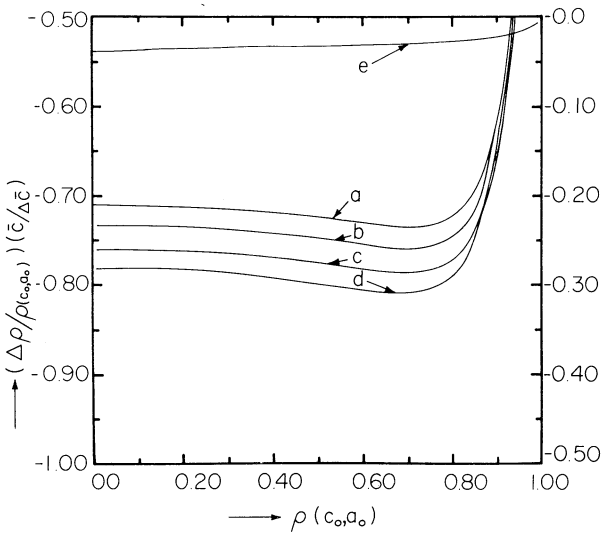

FIG. 2. Plot of $[\Delta\rho/\rho(c_0, a_0)](\bar{c}/\Delta\bar{c})$ vs $\rho(c_0, a_0)$ for various values of (c_0, a_0) and $(\Delta c_0, \Delta a_0)$; $\Delta\rho$ is defined to be $[\rho(c_0 + \Delta c_0, a_0 + \Delta\rho_0) - \rho(c_0, a_0)]$; $\bar{c}$ is $(c_0 + |a_0|)/2$ and $\Delta\bar{c}$ is $(\Delta a_0 + \Delta c_0)/2$. Curve "a" refers to the case $-a_0 = c_0 = 0.60$ and $\Delta a_0 = \Delta c_0 = -0.01$; curve "b" refers to the same as curve "a," except that $\Delta a_0 = \Delta c_0 = +0.01$; curve "c" to the case $-a_0 = c_0 = 0.62$ and $\Delta a_0 = \Delta c_0 = -0.01$; curve "d" refers to the same as curve "c," except that $\Delta a_0 = \Delta c_0 = +0.01$; curve "e" to the case $a_0 = -0.51$, $c_0 = 0.71$, and $\Delta a_0 = \Delta c_0 = -0.1$. The scale on the right refers to curve "e"; the scale on the left refers to the other curves.

racy of this approximation is better than 0.25% for $0.4 < c < 0.8$.

III. ACCURACY REQUIREMENTS

Two factors contribute to the inaccuracy in the derived values of $\rho(z)$, and thus the power spectrum. The first is the statistical error in measuring random quantities. For a normalized correlation function having $\rho(0) = 1$, this error is of order $N^{-1/2}$, where N is the number of independent samples $\simeq Bt$, where B is the full-observing bandwidth and t is the total integration time.

The second factor is the inaccuracy in the computational procedure used to relate r and ρ. This inaccuracy itself arises from two contributions. The first is the inaccuracy caused by the use of an approximation to Eq. (2). The second is that a and c can never be perfectly determined because they will, in general, change during the observation, if only because the system temperature changes as the telescope tracks the source, or the overall system gain changes.

For most astronomical measurements the statistical errors will be much smaller than the computational inaccuracies. How will these errors affect the derived autocorrelation function, and the power spectrum? First, we discuss in a qualitative fashion the errors in the power spectrum which we expect, considering only the first-order effects. Finally, we illustrate the error arising from higher-order effects by making numerical simulations.

a) *Errors in the Assumed Values of the Transition Levels*

The characteristics of Eq. (2) are such that the fractional error in ρ is proportional to the fractional error in c, with a constant of proportionality which depends only insensitively on the value of ρ. This behavior is shown in Fig. 2 for several cases. Figure 2 shows that the fractional errors in ρ and c are proportional except for relatively large values of ρ. In practice, such large values usually occur in the first or second point that has nonzero delay, which we denote by ρ_j, with $j = 1$ or 2. If the assumed value of c is in error, all points of the autocorrelation function other than points with large values are scaled by the same incorrect factor. $\rho(0)$ (hereafter referred to as ρ_0) is defined to be unity and, hence, is not scaled at all. Except perhaps for ρ_1 and ρ_2, and certainly for ρ_0, the *shape* of the autocorrelation function is left unchanged. This means that the shape of the power spectrum is left unchanged, except for the change in shape that results from these three points.

The power spectrum is the cosine Fourier transform of the autocorrelation function. Thus ρ_0 adds a constant to every point on the power spectrum and determines the integral under the power spectrum. Since it is in fact not ρ_0, but all the other points of the autocorrelation function which have a scale error, the net effect on the power spectrum is to change the scale of all of the features in the spectrum, relative to the total integral under the power spectrum. In short, the intensities of all spectral features are in error. Errors in ρ_1 and ρ_2 put a low-order cosine wave through the spectrum, as discussed in Sec. III b.

In the case $-a \neq c$, a similar error occurs. To first-order, the fractional error in ρ is $0.75(-\Delta a/|a| + \Delta c/c)$, and the effect on the power spectrum is similar. Hence, for example, if $\Delta a/|a| = \Delta c/c$, there is no scale error, to the first order.

b) *Errors in the Inversion Approximations*

Figures 1(a) and 1(b), which illustrate the errors in the approximation Eq. (3), show that the maximum errors occur near $|\rho| = 0.86$, the boundary between the ranges of applicability of the two approximations. In practice, ρ_1 and ρ_2 are the only points that may have such a value. Thus, the power spectrum remains correct, except for the contribution of the error of ρ_1 and ρ_2. Since the power spectrum is the cosine Fourier transform of the autocorrelation function, this error adds a low-order cosine wave, $\cos(2\pi jk/N)$, to the power spectrum. Here N is the total number of channels of the correlator; j, as mentioned before, is 1 or 2; and k is a channel number in the power spectrum, $k = 0, 1, \ldots, N-1$. The shapes of narrow spectral features will remain unchanged.

But the effect on real astronomical observations is much smaller. In performing a real astronomical observation, one is interested not in the power spectrum entering the autocorrelator input terminal, but in the power spectrum entering the antenna. Thus, one usually obtains "signal" and "reference" spectra on the sky, and takes the difference. If the difference is small, the two correlation functions are nearly identical and have nearly identical errors; these errors cancel to the first order. In short, errors in the difference spectrum are themselves second-order errors, and are therefore relatively unimportant. To investigate second-order errors, we performed numerical simulations as described in Sec. III c.

c) *Numerical Simulation Studies of "Signal − Reference" Spectra*

We consider the case of a typical observation with a signal and reference spectrum, and illustrate the effects on the difference "signal − reference" spectrum. For the reference spectrum we assumed a spectral shape given by

$$P(f) = T_{\text{noise}}\, H(f),$$

where

$$H(f) = (1/2)\,\{\tanh[q(f/\beta - 1)] - \tanh[q(f/\beta + 1)]\}, \quad (6)$$

which roughly approximates a desirable bandpass shape in an autocorrelation receiver. T_{noise} is the noise temperature of the reference signal, β is the bandwidth, and q is proportional to the slope of the high-frequency edge of the bandpass. For the signal spectrum we assumed a spectral shape given by the reference spectrum, plus a Gaussian line having a height equal to the height of the reference spectrum and a width five times smaller. The signal and reference spectra are shown in Fig. 3. The difference spectrum is relatively large in this case, which should exacerbate the higher-order errors.

The digital sampling rate of the correlator affects our results. We consider two cases. The first is sampling at approximately the Nyquist rate, 2.2β. The second is sampling twice as fast, at 4.4β. In both cases, N, the total number of channels, was set at 128. This more rapid "double Nyquist sampling" is sometimes employed because it provides a slightly improved signal-to-noise ratio (Bowers and Klinger 1974). Double Nyquist sampling produces larger effects, because the time delay of the point ρ_1 or ρ_2 is smaller, and the value of ρ_1 or ρ_2 correspondingly larger. In the two cases, ρ_j for the signal spectrum was approximately 0.2 and 0.7 and j was 2 and 1, respectively.

First, we illustrate the effects that arise from errors in the assumed values of the transition levels discussed in Sec. III a. We first present the case in which the assumed values of the transition levels are (−0.71, 0.71)

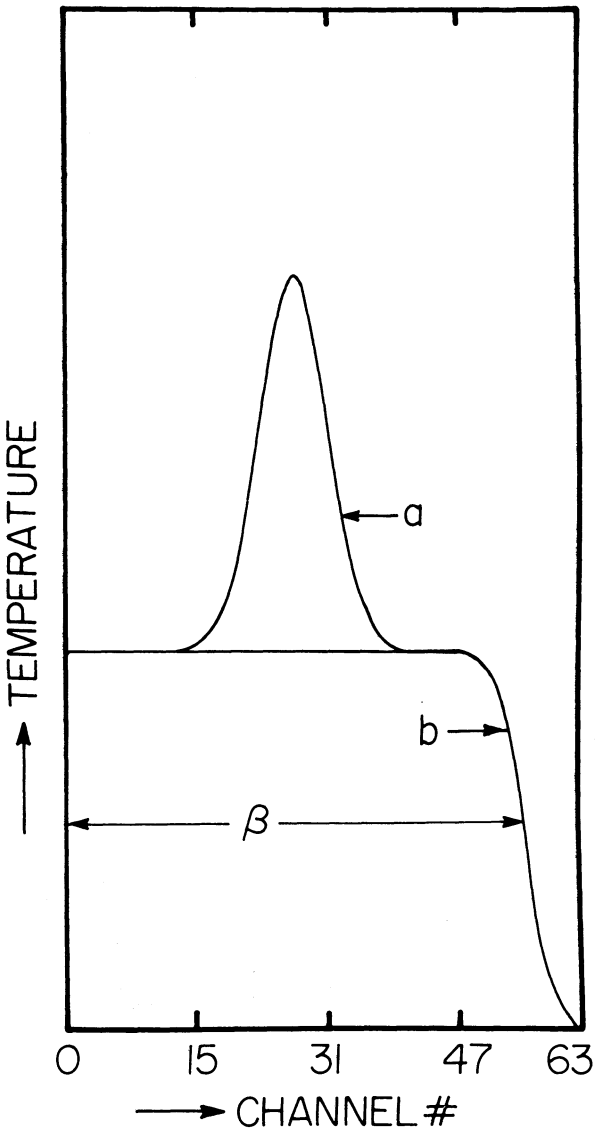

FIG. 3. The references spectrum is curve "b" and curve "a" is the signal spectrum. The bandwidth of the reference is referred to as β in the text; the mid-frequency and the bandwidth of the spectral line are, respectively, 0.5β and 0.2β. q, which describes how sharp the band edge is, has been set equal to 20.0.

when the true values are (−0.61, 0.61), corresponding to $\Delta\bar{c} = 0.1$ in Fig. 2. This case produces larger errors than the corresponding case with $\Delta\bar{c} = -0.1$. Of course, there was an overall scale error of 1.12 in the difference spectrum as discussed in Sec. III a. We illustrate the effects on the shape of the power spectrum in Fig. 4, where we have subtracted the scaled computed difference spectrum from the true difference spectrum; the scale factor was so chosen that the peak of the computed difference spectrum coincided with the peak of the true difference spectrum.

For Nyquist sampling the change in the shape amounts to about 0.04% of the peak of the line, which is

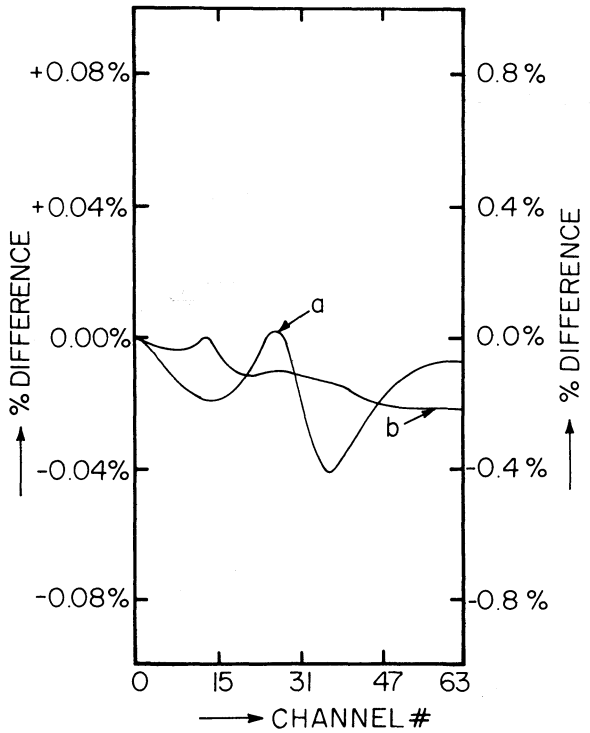

FIG. 4. Plot of the difference between the true spectrum and the computed spectrum, scaled so that the peak of the computed spectrum equals the peak of the true spectrum; further, this difference is expressed as a percentage of the peak temperature of the true line spectrum. The true values of the transition level are −0.61, 0.61; the assumed values are −0.71, 0.71. Curve "a" is the case with a sampling rate of 2.2β; curve "b" is the case with a sampling rate of 4.4β. The scale for curve "a" is the left one and that of curve "b," the right one. In this figure and Figs. 5 and 6, only 64 of the 128 channels are shown; the curves are symmetric about the mid-channel 63.

small—especially considering the fact that a value of $\Delta c = 0.1$ is unrealistically large in practical applications. Double Nyquist sampling increased the error by about an order of magnitude, but the error is still negligible for most practical applications.

In addition, we illustrate in Fig. 5 the case in which the assumed values of the transition levels are (−0.61, 0.61) while the actual values are (−0.51, 0.71). This case, with opposite senses of the error in assumed values of the positive and the negative transition levels, might arise in practice if one arbitrarily assumes that $-a = c$. The results are comparable to the case of Fig. 4.

Finally, we illustrate in Fig. 6 the effects discussed in Sec. III b which arise from errors in our approximation, Eq. (3). Here we take the assumed values of the transition levels equal to the true values, (−0.61, 0.61). As anticipated, the errors are very small, even for double sampling. The error looks like a "baseline" error, of an amount that is far below similar errors which are produced by a multitude of other, more important instrumental effects.

IV. GENERALIZATION TO CROSS CORRELATION FUNCTIONS

Three-level correlators can be cross correlators as well as autocorrelators. This use occurs particularly in interferometry, and also in the quadrature sampling scheme employed in a spectral-line, single-dish correlator at the Hat Creek Radio Observatory. Cross correlation necessitates the use of two digitizers, which may have different transition levels, if only because the gains of the two input signals are different.

Let a_i and c_i be the transition levels of digitizer i, where $i = 1, 2$. Again by a simple extension of the results of Hagen and Farley (1973), one obtains

$$r_{12}(z) - r_{12}(\infty) = \sum_{(a,c)}{}' F(a,c,z), \tag{7}$$

where

$$F(a,c,z) = (2\pi)^{-1} \int_0^{\rho} dx\, (1-x^2)^{-1/2} \times \{\exp[(2acx - a^2 - c^2)/[2(1-x^2)]]\} \tag{8}$$

and

$$r_{ij}(z) = \langle g_i(V_i(t)) g_j(V_j(t+z)) \rangle. \tag{9}$$

The $\Sigma'_{(a,c)}$ stands for summation over the combinations (a_1,c_2), (a_1,a_2), (a_2,c_1), and (c_2,c_1), so that (7) reads

$$r_{12}(z) - r_{12}(\infty) = F(a_1,a_2,z) + F(a_1,c_2,z) + F(a_2,c_1,z) + F(c_2,c_1,z). \tag{7'}$$

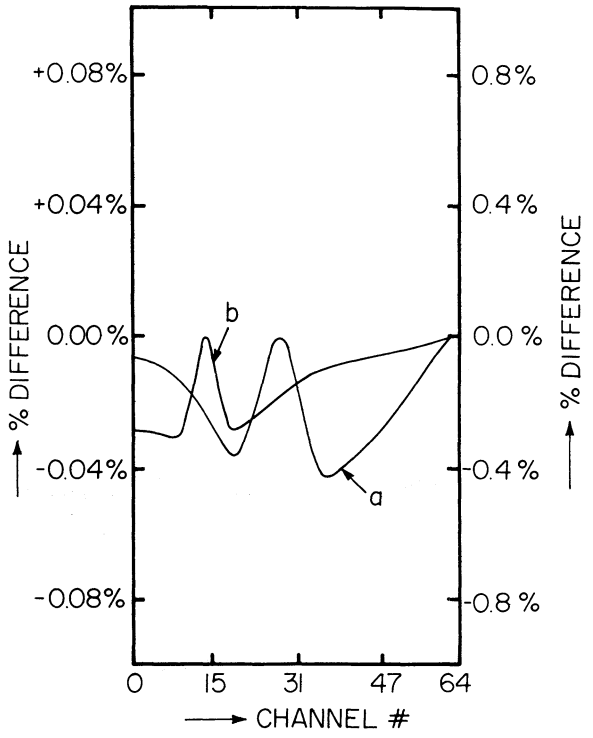

FIG. 5. The same as Fig. 4 except that the assumed values are − 0.51, 0.71.

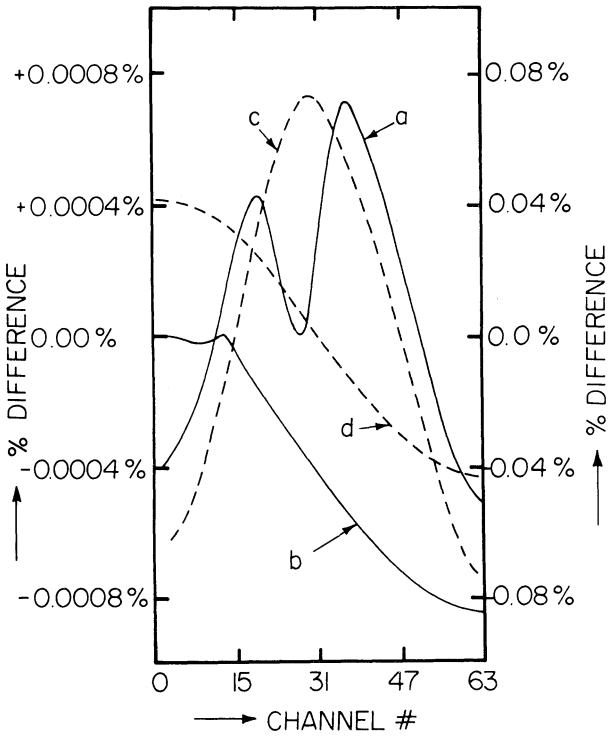

FIG. 6. Curves "a" and "b" are the same scaled differences as in Fig. 4, except that the assumed levels are −0.61, 0.61. The dashed curves represent the differences between the computed spectrum and the true spectrum, expressed as a percentage of the peak temperature of the true line spectrum; however, they are *unscaled*. As discussed in Sec. III b, curve "c," which refers to a sampling rate of 2.2β, is a cosine wave, as is curve "d," which refers to a sampling rate of 4.4β. The scale on the left is for curves "a," "b," and "c" and that on the right is for curve "d."

The inversion of Eq. (7′) is dealt with at length in Appendix A. Section V deals with the problem of determining the four transitional levels.

V. METHODS FOR DETERMINING TRANSITIONAL LEVELS

Let

$$C_i = P(c_i, \infty), \qquad i = 1, 2, \tag{10}$$

$$A_i = p(a_i, -\infty), \qquad i = 1, 2, \tag{11}$$

where $P(a,b)$ is the Gaussian probability that the signal is between levels $a_i\sigma_i$ and $b_i\sigma_i$; then,

$$r_{11}(0) = C_1 + A_1, \tag{12}$$

$$r_{22}(0) = C_2 + A_2, \tag{13}$$

$$r_{11}(\infty) = (C_1 - A_1)^2, \tag{14}$$

$$r_{22}(\infty) = (C_2 - A_2)^2, \tag{15}$$

$$r_{12}(\infty) = (C_1 - A_1)(C_2 - A_2). \tag{16}$$

Note that $r_{12}(\infty)$ simply implies the correlation of two independent, uncorrelated signals, i.e., $\rho_{ij}(\infty) = 0$.

In a system employing quadrature sampling, all the quantities (12) to (16) can, in principle, be determined. Since (7′) is symmetric in upper and lower transition levels, it does not matter whether $A_i > C_i$ or vice versa. Hence, any four of these equations can be solved to obtain A_1, A_2, C_1, C_2. However, one should never assume that $\rho_{ij}(z) = 0$ for any finite value of z, which makes measurement of the levels difficult. One way to circumvent this difficulty is to measure the cross correlation of $V_i(t)$ with a dc signal whose value exceeds $c_i\sigma_i$. Denoting this quantity by r_i, we have

$$r_i = \langle g_i(V_i(t))\, 1 \rangle = C_i - A_i, \qquad i = 1, 2. \tag{17}$$

Now the quantities A_1, A_2, C_1, C_2 can be easily recovered from (12), (13), and (17). Using the normalized Gaussian probability density function, one gets, for example,

$$C_1 = (1/2)[1 - \mathrm{erf}(c_1/\sqrt{2})]. \tag{18}$$

Using the method outlined at the end of Sec. II, c_i can be recovered from C_i. In a similar fashion, the other levels can be recovered.

APPENDIX A

In this section we develop formulas to obtain ρ for a given r in two limits, viz. $\rho \to 0$ and $\rho \to 1$; these will be respectively called the "lower inversion approximation" and the "upper inversion approximation."

First we develop the lower inversion approximation by a simple Taylor expansion of (7′), and obtain

$$F(a,c,z) = (2\pi)^{-1} \sum_{i=0}^{\infty} \phi_{(i)}(a,c,)\rho^{i+1}, \tag{A1}$$

where

$$\phi_{(i)}(a,c) = [1/(i+1)!] \sum_{j=0}^{i} f_{(i-j)} g_{(j)}\, {}^iC_j,$$

$${}^iC_j = i!/j!(i-j)! \tag{A2}$$

and

$$g_{(i+1)} = \sum_{k=0}^{i} h_{(k+1)} g_{(i-k)}\, {}^iC_k, \quad g_{(0)} = e^{\alpha}, \tag{A3}$$

with

$$1/(1-x^2)^{1/2} = \sum_{i=0}^{\infty} (f_{(i)}/i!)x^i. \tag{A4}$$

The g's are the coefficients of the series obtained by expanding the expression in the curly brackets of (8) about $\rho = 0$; for example $f_{(0)} = 1, f_{(2)} = 1, f_{(4)} = 9, f_{(6)} = 225$, $f_{(2j+1)} = 0$; $h_{(2j)} = (2j)!\alpha$, $h_{(2j+1)} = -(2j+1)!\beta$; where $\alpha = -\frac{1}{2}(a^2 + c^2)$ and $\beta = -ac$, and $j = 0, 1, 2, \ldots$. Using (7′) and (A1) to (A4), we get

$$y(z) = r(z) - r(\infty) = \sum_{i=1}^{\infty} \psi_{(i)}\rho^i, \quad \text{(A5)}$$

where

$$\psi_{(i)} = \sum_{(a,c)}{}' \phi_{(i-1)}(a,c). \quad \text{(A6)}$$

It is necessary to invert the series (A5) in order to obtain the lower inversion formula. This can be achieved with the help of a standard formula for inverting a series, for example, Abramowitz and Stegun (1972, p. 16); hence,

$$\rho(z) = \sum_{i=1}^{N} \theta_{(i)} y^i(z), \quad \text{(A7)}$$

where

$$\theta_{(1)} = 1/\psi_{(1)}; \theta_{(2)} = -\psi_{(2)}/\psi_{(1)}^3; \theta_{(3)} = (3\psi_{(2)}^2 - \psi_{(1)}\psi_{(3)})/\psi_{(1)}^5, \text{ etc.} \quad \text{(A8)}$$

and N is the order of approximation.

Next, we consider the upper inversion approximation. Here we restrict our consideration to the autocorrelation case, i.e., $a_2 = a_1$ and $c_2 = c_1$, since, in practice, the cross correlation is rarely near unity. Changing the lower limit from 0 to 1 in (7′), one obtains

$$r(0) - r(z) = 2G(a,c,z) + G(a,a,z) + G(c,c,z), \quad \text{(A9)}$$

where

$$G(a,c,z) = (2\pi)^{-1} \int_{\rho(z)}^{1} dx(1-x^2)^{-1/2} \times \exp\{(2acx - a^2 - c^2)/[2(1-x^2)]\} \quad \text{(A10)}$$

and

$$G(a,a,z) = (2\pi)^{-1} \int_{\rho(z)}^{1} dx(1-x^2)^{-1/2} \times \exp[-a^2/(1+x)]. \quad \text{(A11)}$$

Recasting the expression in the square brackets of (A11), (A11) can be written as

$$G(a,a,z) = [\exp(-a^2/2)/2\pi] \int_{\rho(z)}^{1} dx \times (1-x^2)^{-1/2} \exp(-a^2t^2/2), \quad \text{(A12)}$$

where

$$t^2 = (1-x)/(1+x). \quad \text{(A13)}$$

Expansion of the exponential in powers of t^2, subsequent integration of the terms, and retention of the first four terms of the expansion of $\tan^{-1}(t)$ results in

$$G(a,a,z) = [\exp(-a^2/2)/2\pi][\cos^{-1}\rho + a^2(-t^3/3 + t^5/5 - t^7/7) + (a^4/4)(t^5/5 - t^7/7) + (a^6/24)(-t^7/7)], \quad \text{(A14)}$$

where

$$t^2 = (1-\rho)/(1+\rho). \quad \text{(A15)}$$

Recasting the expression in the square brackets of (A10), (A10) can be written as

$$G(a,c,z) = (2\pi)^{-1} \int_{\rho(z)}^{1} dx(1-x^2)^{-1/2} \times \exp\{-ac/(1+x) - 2\lambda/[(1-x)(1+x)]\}, \quad \text{(A16)}$$

where

$$\lambda = (a-c)^2/4. \quad \text{(A17)}$$

Approximating $(1+x)$ by 2, (A16) becomes

$$G(a,c,z) = (2\pi)^{-1} \int_{\rho(z)}^{1} dx[2(1-x)]^{-1/2} \times \exp[-(ac/2) - \lambda/(1-x)]. \quad \text{(A18)}$$

By transformation $t^2 = \lambda/1 - x$, (A18) reduces to

$$G(a,c,z) = (1/\pi)(\lambda/2)^{1/2} \exp(-ac/2) \times \{\exp(-t)/t^{1/2} - \pi^{1/2}[1 - \text{erf}(t^{1/2})]\}, \quad \text{(A19)}$$

where

$$t = \lambda/(1-\rho). \quad \text{(A20)}$$

The error function can be evaluated by any of the numerical approximations, such as that in Abramowitz and Stegun (1972, p. 299). (A9), (A14), (A15), (A19), and (A20) can be combined to give rise to a transcendental equation in $r(z)$. To solve for $r(z)$, any standard method such as the Newton-Raphson method can be used. If only the first term of (A14) and none of the terms of (A19) are retained, then (A9) can be inverted to give $\rho(z)$ quite easily; we call this approximation, (A21), the upper inversion formula of order zero:

$$\rho(z) = \cos\{2\pi[r(0) - r(z)]/[\exp(-a^2/2) + \exp(-c^2/2)]\}. \quad \text{(A21)}$$

In all of these equations of the upper inversion formula, viz. (A9) to (A21), the absolute value of $r(z)$ should be used; the sign of $\rho(z)$ naturally is the sign of $r(z)$. Note that (A21) is a poor approximation for the case $-a = c = 0$; this is due to our neglect of all the terms of (A19) in (A9). We thank Dr. Jerry Hudson of the Space Sciences Laboratory, University of California at Berkeley for drawing our attention to this failure.

APPENDIX B

For the reader's convenience, we quote below a numerical approximation to the error function (Hastings 1966):

$$\text{erf}(x) = (2/\sqrt{\pi}) \int_0^{\infty} dx \exp(-x^2) = 1 - (a_1\eta + a_2\eta^2 + a_3\eta^3 + a_4\eta^4 + a_5\eta^5) \times \exp(x^2) + \epsilon(x), \quad \text{(B1)}$$

where

$$\eta = 1/(1 + \rho x),\ \rho = 0.327\,591\,1,$$
$$a_1 = 0.254\,829\,592,\ a_2 = -0.284\,496\,736,$$
$$a_3 = 1.421\,414\,137\,41,\ a_4 = -1.453\,152\,027,$$
$$a_5 = 1.061\,405\,429,\ |\epsilon(x)| \leq 1.5 \times 10^{-7}.$$

APPENDIX C

We have also worked out the upper and lower inversion approximations for a 1-bit (i.e., 2-level) by 3-level correlator, a type which is used at some observatories. The integral relation connecting r to ρ has been worked out by Hagen and Farley (1973). However, the relation given by these authors is incorrect. The correct relation is

$$r = \left(\frac{2}{\pi}\right) \int_0^{\rho} dx\ [1/(1 - x^2)^{1/2}] \times \exp\{[-c^2/[2(1 - x^2)]\}. \quad \text{(C1)}$$

By essentially identical application of the methods developed in Appendix A, the lower inversion approximation of order 3 and an upper inversion approximation have been obtained. These are, respectively,

$$|\rho| = A|r| + B|r|^3, \quad \text{(C2)}$$

where

$$A = (\pi/2)\exp(c^2/2),$$
$$B = -[(c^2 + 1)/6]A^3$$

and

$$|r| - r_0 = \left(\frac{2}{\pi}\right)(2\lambda)^{-1/2}\exp(-t^2)/t - \sqrt{\pi}\,[1 - \mathrm{erf}(t)], \quad \text{(C3)}$$

where

$$t = [\lambda/(1 - |\rho|)]^{1/2},$$
$$r_0 = r(0) = 1 - \mathrm{erf}(c/\sqrt{2}). \quad \text{(C4)}$$

As before, the sign of ρ follows that of r. The lower inversion approximation is accurate to better than 2% for $0 < |\rho| < 0.4$ with $c = 0.65$. The representation for r is good for $1 < |\rho| < 0.95$ with $c = 0.65$.

REFERENCES

Abramowitz, M., and Stegun, I. (1972). *Handbook of Mathematical Functions* (Dover, New York).

Bowers, F. K., and Klinger, R. J. (1974). Astron. Astrophys. Suppl. **15,** 373.

Cooper, B. F. C. (1970). Aust. J. Phys. **8,** 115.

Hagen, J. B., and Farley, D. T. (1973). Radio Sci. **8,** 775.

Hastings, C. (1966). *Approximations for Digital Computers* (Princeton University, Princeton).

Thompson, A. R. (1973). VLA Electronics Memorandum No. 112.